Cofactor and Substrate Binding to Vanadium Chloroperoxidase Determined by UV−VIS Spectroscopy and Evidence for High Affinity for Pervanadate†

Rokus Renirie,‡ Wieger Hemrika,‡ Sander R. Piersma,§ and Ron Wever*,‡

E.C. Slater Institute, Biocentrum Amsterdam, University of Amsterdam, Plantage Muidergracht 12, 1018 TV Amsterdam, The Netherlands, and Center for Protein Technology, TNO-WU, Wageningen University, Bomenweg 2, 6703 HD Wageningen, The Netherlands

Received September 20, 1999; Revised Manuscript Received November 5, 1999

ABSTRACT: The vanadate cofactor in vanadium chloroperoxidase has been studied using UV−VIS absorption spectroscopy. A band is present in the near-UV that is red-shifted as compared to free vanadate and shifts in both position and intensity upon change in pH. Mutation of vanadate binding residues has a clear effect on the spectrum. Substrate-induced spectral effects allow direct measurement of separate kinetics steps for the first time for vanadium haloperoxidases. A peroxo intermediate is formed upon addition of H_2O_2, which causes a decrease in the absorption spectrum at 315 nm, as well as an increase at 384 nm. This peroxo form is very stable at pH 8.3, whereas it is less stable at pH 5.0, which is the optimal pH for activity. Upon addition of halides to the peroxo form, the native spectrum is re-formed as a result of halide oxidation. Stopped-flow experiments show that H_2O_2 binding and Cl^- oxidation occur on the millisecond to second time scale. These data suggest that the oxidation of Cl^- to HOCl occurs in at least two steps. In the presence of H_2O_2, the affinity for the vanadate cofactor was found to be much higher than previously reported for vanadate in the absence of H_2O_2. This is attributed to the uptake of pervanadate by the apo-enzyme. Human glucose-6-phosphatase, which is evolutionarily related to vanadium chloroperoxidase, is also likely to have a higher affinity for pervanadate than vanadate. This could explain the enhanced insulin mimetic effect of pervanadate as compared to vanadate.

Vanadium chloroperoxidase (VCPO)[1] from the fungus *Curvularia inaequalis* belongs to the group of haloperoxidases which catalyze the two-electron oxidation of a halide to the corresponding hypohalous acid according to

$$H_2O_2 + H^+ + X^- \rightarrow H_2O + HOX$$

These haloperoxidases are named after the most electronegative halide they are able to oxidize, and thus a chloroperoxidase is able to oxidize chloride, bromide, and iodide. The class of vanadium-containing haloperoxidases (VHPO's) bind vanadate (HVO_4^{2-}) as a prosthetic group. During turnover, the transition metal in these vanadate-containing haloperoxidases does not change its redox state but is proposed to function as a Lewis acid (*1*, *2*). In contrast, heme-containing haloperoxidases catalyze the formation of the hypohalous acid by a redox mechanism in which iron is oxidized and reduced during catalysis. In the Lewis-acid mechanism, H_2O_2 is first activated by binding to the metal after which the halide is oxidized.

The crystal structure of vanadium chloroperoxidase (VCPO) from *C. inaequalis* shows that the HVO_4^{2-} cofactor is covalently attached to $N^{\epsilon 2}$ of His496, while five residues (Arg360, Arg490, Lys353, Ser402, and Gly403) donate hydrogen bonds to the nonprotein oxygens. The resulting structure is a trigonal bipyramid (Figure 1A) with three nonprotein oxygens in the equatorial plane. The fourth oxygen (hydroxide group) and the nitrogen from His496 are at the apical positions of the pyramid. The affinity of the apo-enzyme for vanadate is considerable; a dissociation constant as low as 100 nM has been reported (*3*), which increases below pH 6. The above-mentioned vanadate binding residues were shown to be conserved in several acid phosphatases (*4*−*6*), among others the membrane-bound human glucose-6-phosphatase (G6Pase), a key enzyme in gluconeogenesis. Phosphatase activity as determined for vanadate-free chloroperoxidase (*6*) confirmed the suggestion that the active sites of these enzymes are similar. This similarity led to the assignment of putative roles of corresponding residues in G6Pase (*6*) and consequently to a reevaluation of its transmembrane topology (*7*, *8*). VCPO can in fact be regarded as a phosphatase with the transition-state analogue vanadate found at the active site.

Recently, site-directed mutagenesis studies have been performed on cofactor binding residues of VCPO (*9*), showing the importance of the binding residue His496 and positively charged residues surrounding the cofactor. It was

† This work was supported by the Council of Chemical Sciences of the Netherlands Organization for Scientific Research and was made possible by financial support from the Netherlands Organization for Scientific Research, the Netherlands Technology Foundation (STW), and the Netherlands Association of Biotechnology Centres (ABON).

* To whom correspondence should be addressed. Tel: +31 (20) 525 5110. Fax: + 31 (20) 525 5124. E-mail: a311rw@chem.uva.nl.

‡ University of Amsterdam.

§ Wageningen University.

[1] Abbreviations: VCPO, vanadium chloroperoxidase; rCPO, recombinant chloroperoxidase; VHPO, vanadium haloperoxidase; MCD, monochlorodimedone; G6Pase, glucose-6-phosphatase.

10.1021/bi9921790 CCC: $19.00
Published on Web 01/13/2000

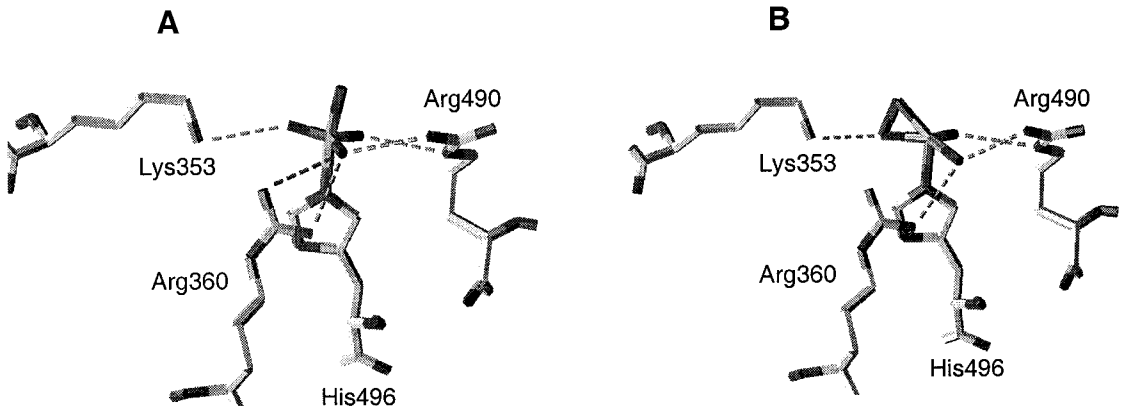

FIGURE 1: Trigonal bipyramidal native form (A) and distorted tetragonal peroxide form (B) of VCPO as determined by X-ray crystallography. Additionally, the cofactor binding residues His496, Arg490, Arg360, and Lys353 are shown.

suggested that these positively charged residues not only compensate for the negative charge of the cofactor but also help to activate the bound peroxide prior to halide attack. A determination of the X-ray structure of the peroxide derivative of the enzyme (*10*) shows a geometry with the peroxide bound in a side-on fashion. It can be regarded as a distorted tetragonal pyramid (Figure 1B) with the two peroxide oxygens, one oxygen, and the His496 nitrogen in the basal plane and one oxygen in the apical position.

The vanadium haloperoxidases are colorless, hampering spectroscopic studies. EPR has been used to characterize the inactive reduced vanadium(IV) form of the enzyme (*11*). In addition, vanadium bromoperoxidase (VBPO) from the seaweed *Ascophyllum nodosum* has been characterized by EXAFS (*2*, *12*), and clear differences in edge and preedge features are observed after addition of H_2O_2. EXAFS studies on recombinant VCPO give similar results and yield detailed vanadium−oxygen distances in the native and peroxide form (unpublished results). However, EXAFS requires very high concentrations (~1 mM), and determination of kinetic parameters is impossible. For VBPO from *A. nodosum*, a small difference in the UV spectrum at 315 nm between apo- and holo-enzyme was observed (*13*) which was influenced by H_2O_2 and bromide, but no detailed studies on this feature were reported. In the visible region of the electromagnetic spectrum, free vanadate does not show transitions although a yellow color is observed for some vanadium(V) solutions (*14*), due to absorption tailing from the UV. Several multimeric species may be present, and therefore the UV spectra of vanadate depend strongly on pH and vanadate concentration. These spectra have low extinction coefficients and are found below 350 nm.

Here we show that it is possible to study the bound cofactor in VCPO and the effects of addition of H_2O_2 and halides in detail by using UV−VIS absorption spectroscopy. By stopped-flow spectroscopy, we have been able to obtain the second-order rate constant for binding of H_2O_2 and the rate constant for Cl^- oxidation, and the consequences of these measurements for the catalytic mechanism are discussed. Also, the effects of mutation of vanadate binding residues on the optical absorbance band are described.

Further, we show that the apo-enzyme has an increased affinity for the vanadate cofactor in the presence of its substrate H_2O_2, and the effects of mutation of vanadate binding residues on the affinity for vanadate in the presence of H_2O_2 are presented. The possible implications of the putative high affinity of the evolutionary related human glucose-6-phosphatase and other phosphatases for pervanadate (the complexes of vanadate with H_2O_2) are discussed. Our results strengthen the hypothesis that the insulin mimetic effects of vanadate-derived drugs are partially due to inhibition of glucose-6-phosphatase (*15*, *16*).

EXPERIMENTAL PROCEDURES

Production and Isolation of rCPO and Mutant Enzymes. The production and isolation of rCPO, H496A, R490A, R360A, and K353A are described in detail elsewhere (*9*). The crystal structure of rCPO is very similar to that of the enzyme from *C. inaequalis*, especially the active site (*17*). Also, the specific activities of rCPO for Cl^- and Br^-, $K_m(Cl^-)$, $K_m(Br^-)$, and $K_m(H_2O_2)$ at pH 5.0 are identical (*9*). rCPO is produced as apo-enzyme by the yeast expression system, and the apo-enzyme from *C. inaequalis* was formed by dialyzing the holo-CPO against 100 mM phosphate−citrate buffer, pH 3.8, containing 1 mM EDTA and further dialysis against the desired buffer. The relative amount of apo-enzyme was larger than 99% for both *C. inaequalis* CPO and rCPO as determined by comparison of the activity of the preparations in the absence and presence of 100 μM vanadate in the activity assay.

Optical Absorbance Spectra. UV−visible absorption spectra were taken on a Hewlett-Packard 8452A diode array spectrophotometer (2 nm resolution) except for the inset in Figure 2, which was taken on a Cary 50 spectrophotometer (0.5 nm resolution). Enzyme solutions were buffered in 100 mM Tris−HAc buffer, pH 5.0 and 8.3. Prior to measurement, enzyme solutions were centrifuged for 10 min at 13 000 rpm in an MSE MicroCentauer centrifuge to eliminate absorption by any denatured protein.

Stopped-Flow Experiments. Stopped-flow absorbance experiments were performed with an Applied Photophysics SX.18MV spectrometer (dead time 1.5 ms) maintained at 10 ± 0.5 °C with a Lauda RM6 cryostat. The SX.18MV stopped-flow apparatus can operate in the sequential mixing mode, allowing a premixing step followed by an aging time (milliseconds to seconds) before the actual mixing with the third reagent in the observation cell takes place. In the chloride oxidation experiments, enzyme was premixed with H_2O_2, and after a delay of 3 s in which the binding of H_2O_2 is complete and less than 5% of the native enzyme is re-

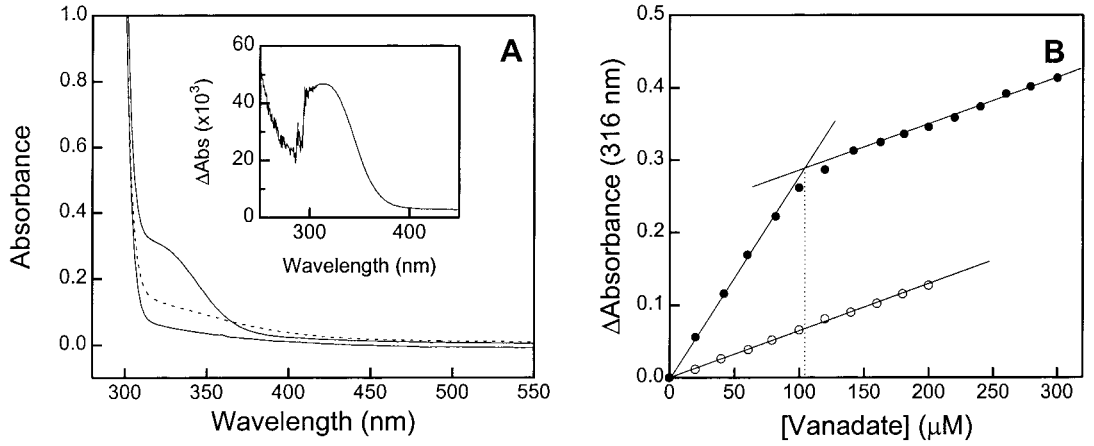

FIGURE 2: Panel A: UV−VIS absorption spectra of 100 μM chloroperoxidase at pH 8.3. The lower solid line shows the apo-enzyme, the upper solid line the holo-enzyme formed after addition of 100 μM vanadate, and the dotted line the spectrum after addition of 100 μM H_2O_2. The inset shows the difference spectrum for 16 μM holo-CPO minus apo-CPO, showing a maximum at 315 nm. Panel B: Titration of apo-CPO with vanadate: changes in the optical absorbance at 316 nm. (●) Absorbance change of 100 μM apo-CPO induced by vanadate. (○) Absorbance of free vanadate.

formed, it was mixed with various amounts of Cl^- (final enzyme concentration: 50 μM). Kinetic traces were fitted using software supplied by the apparatus. Enzyme, H_2O_2, and Cl^- solutions were made in 100 mM Tris−HAc buffer, pH 5.0 and 8.3.

Enzyme Activity Assays. Haloperoxidase activity was measured by measuring the chlorination/bromination of monochlorodimedone (MCD, $\Delta\epsilon = 20.1$ mM^{-1} cm^{-1} at 290 nm). To assess cofactor binding, the activity of each mutant was assayed at optimal substrate concentrations at pH 6.2 (50 mM citrate) as determined from steady-state measurements (*9*): K353A, 10 mM H_2O_2 and 40 mM Br^-; R360A, 40 mM H_2O_2 and 20 mM Br^-; R490A, 40 mM H_2O_2 and 20 mM Br^-.

Miscellaneous. rCPO was concentrated using the Centricon-30 and Microcon-30 system from Amicon. Protein concentration was determined using the Bradford assay (*18*), and H_2O_2 concentration was determined using a molar extinction coefficient of 43.6 M^{-1} cm^{-1} at 240 nm. Stocks were prepared daily.

RESULTS

Optical Absorbance Spectra. The native *C. inaequalis* system produces low amounts of vanadium chloroperoxidase which after isolation contains nonprotein dyes. These are believed to adhere to the surface of the enzyme, giving rise to a brownish color, which becomes quite intense above protein concentrations of 1 mg/mL and makes sensitive optical spectroscopy impossible. In contrast, the *S. cerevisiae* recombinant system allows the production of large amounts of very pure enzyme which, even at concentrations of 100 mg/mL, are colorless, allowing optical spectroscopic studies on this enzyme. Figure 2A shows the optical spectra of apo-rCPO and holo-rCPO and the effect of H_2O_2 addition at pH 8.3. A clear difference is observed between the spectra of holo- and apo-enzyme, with a peak at 315 nm. The absorption at 315 nm is not due to the absorption of free vanadate since this has a lower extinction coefficient, as illustrated in Figure 2B. Titration of apoprotein with vanadate in the range of 0−100 μM resulted in a linear absorbance increase with $\epsilon = 2.8$ mM^{-1} cm^{-1}. At concentrations higher than 100 μM vanadate, the absorbance increase is less and

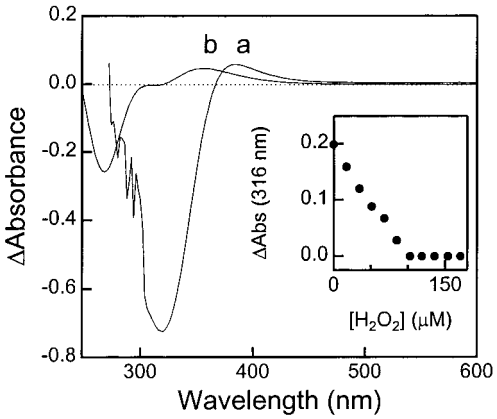

FIGURE 3: (a) Difference spectrum for 300 μM peroxo-CPO minus holo-CPO. (b) Difference spectrum for 300 μM pervanadate minus vanadate. Inset: Titration of 100 μM holo-rCPO with H_2O_2 at pH 8.3.

is identical to that of free vanadate, strongly suggesting stoichiometric binding of vanadate to the apo-rCPO. Assuming stoichiometric binding of vanadate, it was possible to calculate an extinction coefficient of 90 mM^{-1} cm^{-1} at 280 nm for apo-rCPO, giving an $A_{315\ nm}/A_{280\ nm}$ ratio of 0.03. The noise in the difference spectrum at lower wavelength is caused by the strong background absorption at 280 nm.

Crystallographic data show the formation of a peroxo intermediate when H_2O_2 is added to crystals of VCPO (*10*). Interestingly, the addition of H_2O_2 has a clear effect on the intensity of the observed optical band, resulting in a significant decrease of the 315 nm absorption band, which most likely reflects the formation of the peroxo intermediate observed in the crystal structure. A small absorbance with $\epsilon = 0.7$ mM^{-1} cm^{-1} at 315 nm is still present (Figure 2A). Figure 3a shows the difference spectrum of 300 μM peroxo- minus holo-CPO. The peroxo form of the enzyme shows a small peak at 384 nm. This absorbance is clearly red-shifted as compared to the difference spectrum of pervanadate minus vanadate (354 nm; Figure 3b). The patterns of spectra a and b are similar, with a large negative peak and a small positive peak. The negative peak is also red-shifted (315 vs 268 nm). Addition of H_2O_2 to the apo-enzyme had no effect on the spectrum (not shown). The inset shows the titration of the

holo-enzyme (100 μM) with H_2O_2. The absorbance decrease was monitored at 316 nm, and a 1:1 stoichiometry between the enzyme and H_2O_2 concentration is observed. The sharp point of intersection indicates a binding constant less than 20 μM, which is in line with the estimated K_m value for H_2O_2 at this pH (<1 μM) (*3*). The peroxo intermediate is stable for at least 1 h, but when 1 mM Cl^- was added, turnover was induced and the spectrum of the holo-enzyme was recovered within 10 min (not shown). This slow recovery of the original spectrum is in line with the high K_m value for chloride and low turnover number at this pH (*11*).

At pH 5.0, the optimal pH for chloroperoxidase activity, the optical spectra and substrate-induced changes are similar to those seen at pH 8.3 (not shown), but details are different. Addition of 100 μM vanadate to 100 μM apo-rCPO results in the immediate formation of an optical band which differs in intensity and position from those of free vanadate at this pH. Titration of 100 μM apo-rCPO with 0−300 μM vanadate gives an identical pattern as in Figure 2B (not shown). However, the peak position of the optical band is shifted toward 305−310 nm. Its position is difficult to determine exactly because of the high background absorbance. The extinction coefficient of the band has decreased to about 2.0 mM^{-1} cm^{-1} at 308 nm. Addition of 100 μM H_2O_2 to the holo-enzyme results in a similar decrease of the band as observed at pH 8.3. However, the native spectrum is re-formed spontaneously within 5 min. It is conceivable that this is due to catalase activity. However, a second addition of 100 μM H_2O_2 results in a spectrum with a larger decrease in absorbance as observed for the first addition but now the intermediate is stable for at least 10 min. It is possible that trace amounts of halides are the cause of the instability, since VCPO has much lower K_m values and a much higher turnover for halides at pH 5.0 than at pH 8.3 (*11*, *19*). To test this hypothesis, a substoichiometric amount of 20 μM Cl^- was added after the second addition of H_2O_2. In this respect, it is important to note that the halide in principle can act catalytically, because of the following reaction (*20*−*22*) in which the halide is formed again:

$$HOX + H_2O_2 \rightarrow {}^1O_2 + X^- + H_2O$$

Indeed, the low amount of Cl^- was capable of completely returning the peroxo intermediate to the native spectrum within 5 min. After recovery of the native spectrum, another addition of H_2O_2 again leads to a stable intermediate, indicating that the free halide is now removed. We assume that the formed HOX not only is reacting with H_2O_2 but also is slowly scavenged by buffer components (*23*) or by amino acid residues, both resulting in the removal of free halide.

Stopped-Flow Experiments. At pH 8.3, mixing of 50 μM enzyme with 50 μM H_2O_2 results in a very rapid decay of the absorption of the native enzyme, with 90% of the peroxo intermediate formed within 20 ms (not shown). The kinetics trace was fitted to a hyperbola, which is the result expected for a second-order reaction when the initial concentrations of enzyme and substrate are the same. The observed absorbance decrease is in agreement with the extinction coefficient of holo minus peroxo CPO as determined from Figure 2A. The very rapid formation of the peroxo intermediate at this pH makes it very difficult to measure this rate under pseudo-first-order conditions. However, at pH 5.0 the rate of formation is much slower as can be observed in Figure 4A. Slow decay of the peroxo state to the native state is also observed (Figure 4B). This latter process was fitted with a single-exponential function giving a first-order rate constant of 0.013 s^{-1}. In Figure 5, a typical kinetics trace for the formation of the peroxo intermediate obtained under pseudo-first-order conditions is shown, fitted with a single-exponential function. The inset shows the linear relation between the observed rate constants and H_2O_2 concentration, according to eq 1 and assuming the minimal Scheme 1 (*24*):

$$k_{obs} = k_{-1} + k_1[H_2O_2] \quad (1)$$

Here k_{obs} is the observed rate constant. At this pH and

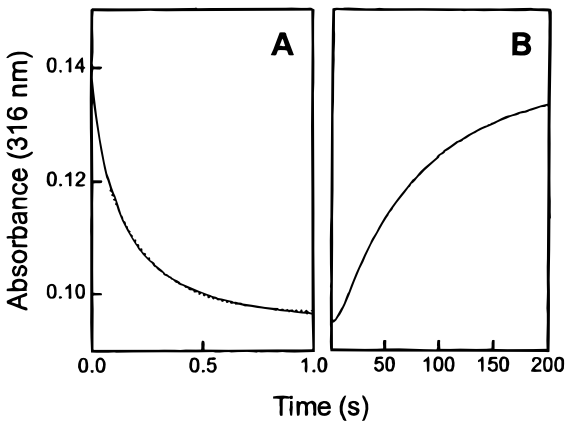

FIGURE 4: Panel A: Stopped-flow progress curve for mixing equimolar concentrations of VCPO and H_2O_2 at pH 5.0. The kinetics trace shows the formation of the peroxo intermediate. A hyperbolic fit is also shown. Panel B: Decay of the peroxo intermediate and slow re-formation of the native enzyme at pH 5.0. The latter was fitted with a single-exponential function. Conditions: 50 μM VCPO and 50 μM H_2O_2.

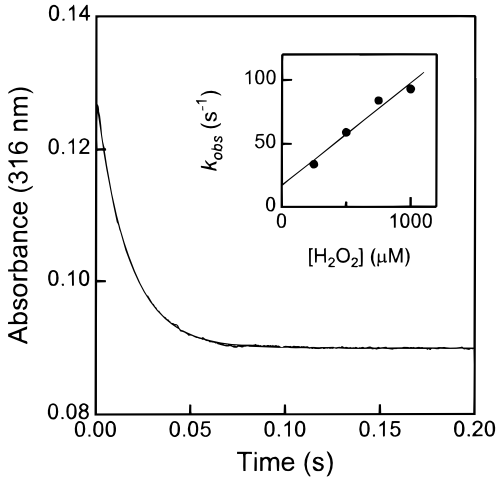

FIGURE 5: A typical progress curve for the reaction of VCPO with H_2O_2 under pseudo-first-order conditions at pH 5.0. A single-exponential fit is shown. Conditions: 50 μM VCPO and 500 μM H_2O_2. Inset: the observed rate constant for the binding of H_2O_2 to VCPO as a function of the H_2O_2 concentration at pH 5.0. Data were obtained from single-exponential fits.

Scheme 1

$$\text{CPO} + H_2O_2 \underset{k_{-1}}{\overset{k_1}{\rightleftharpoons}} \text{Peroxo-CPO}$$

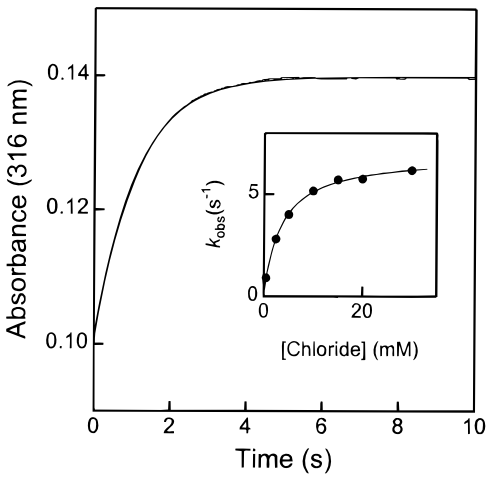

FIGURE 6: Stopped-flow progress curve for the oxidation of chloride by the peroxo intermediate of VCPO at pH 5.0 under pseudo-first-order conditions. Enzyme was premixed with H_2O_2, and after a delay of 3 s, it was mixed with Cl^-. Final conditions after sequential mixing: 50 μM peroxo intermediate and 0.5 mM Cl^-. A single-exponential fit is shown. Inset: the observed rate constant for chloride oxidation as a function of chloride concentration.

Scheme 2

$$\text{Peroxo-CPO} + Cl^- \underset{k_{-2}}{\overset{k_2}{\rightleftharpoons}} \text{"CPO-HOCl"} \xrightarrow{k_3} \text{CPO} + \text{HOCl}$$

temperature, the second-order rate constant k_1 for the association of enzyme and H_2O_2 is 0.8×10^5 M^{-1} s^{-1}. This value is in agreement with $k_{cat}/K_m = 1.2 \times 10^5$ M^{-1} s^{-1} as determined from steady-state measurements under the same conditions, fitted with the program LEONORA (*25*) (not shown).

It was also possible to study chloride oxidation. This was achieved by premixing enzyme and H_2O_2, and, after a short delay, the formed peroxo intermediate was mixed with chloride. A kinetics trace under pseudo-first-order conditions at 10 °C and a single-exponential fit are shown in Figure 6. The inset shows the observed rate constant plotted as a function of chloride concentration. The observed rate constant shows a clear nonlinear dependence on the chloride concentration. Data were fitted to the hyperbolic eq 2 (*24*):

$$k_{obs} = k_3[Cl^-]/(K_S + [Cl^-]) \quad (2)$$

where $K_S = k_2/k_{-2}$. Scheme 2 gives a possible sequence of events, involving a fast preequilibrium between the peroxo intermediate and Cl^- before HOCl is released. The calculated k_3 (7.0 s^{-1}) is similar in magnitude to the measured k_{cat} from steady-state kinetics (10 s^{-1}).

Optical Absorbance Spectra of Mutant CPO's. To test whether mutation of the vanadate binding or coordinating residues has an effect on the observed absorbance spectrum, mutants of His496, Arg360, Arg490, and Lys353 were investigated at pH 8.3. The crystal structure of H496A shows that at a high concentration of vanadate (1 mM) vanadate is still present in the active site, despite the absence of the covalent bond to His496 (*17*). Addition of 0−2.4 mM vanadate to 100 μM apo-H496A did not result in the formation of an optical band in the 300−400 nm region, indicating the importance of His496 for the optical band. Interestingly, in mutants R490A and K353A (for which crystal structures are not available yet), the optical band was also not formed upon addition of 0−0.5 mM vanadate (not shown). Mutant R360A did show an optical absorption band with an absorption maximum shifted to 305−310 nm and with a lowered extinction coefficient of 1.5 mM^{-1} cm^{-1} at 308 nm (not shown). Titration of 100 μM apo-R360A with 0−300 μM vanadate showed stoichiometric binding, indicative of a small value for the dissociation constant for vanadate of this mutant (<20 μM). The crystal structure of R360A (*17*) shows that the vanadate ion is still covalently bound to His496, indicating that this bond is important both for the strength of binding and for the presence of the optical band.

Affinity of CPO for Vanadate in the Absence and Presence of Substrate H_2O_2. Based on the linear relationship between absorbance changes and the vanadate concentration, an upper limit for the dissociation constant for vanadate of about 20 μM can be estimated from our data; a more precise determination is not possible due to the small differences in absorbance at lower enzyme concentrations. Classically, one would determine the dissociation constant of the cofactor in vanadium haloperoxidases by preincubation of apo-enzyme with various amounts of vanadate at different pH values, and measuring the activities of samples in an activity assay at optimal pH. In this approach, one assumes a linear relationship between the amount of bound vanadium and activity (*11*), and further it assumes that within the time of activity measurement the dissociation equilibrium is not affected by dilution and pH change, resulting in linear traces during activity measurements. Using this method, a dissociation constant of about 100 nM at pH 8.3 was reported (*3*), a value in line with the upper limit estimated from Figure 2. At pH 5.0, the dissociation constant was reported to be larger than 1 μM (*3*).

Surprisingly, in this classical approach we observed an increase of activity in time at low concentrations of vanadate, which was not reported previously (*3*). This activation during turnover was independent of pH of preincubation and time of preincubation. A likely explanation is that the presence of substrates during turnover shifts the equilibrium of vanadate binding and therefore increases the uptake of cofactor. This hypothesis was further tested using low amounts of apo-enzyme and cofactor, and the result is shown in Figure 7. Using 10 nM apo-enzyme and 10 nM vanadate, less than 1% of cofactor is expected to bind at this pH, assuming a dissociation constant higher than 1 μM (*3*). Trace a shows activation of apo-rCPO during turnover. Trace b shows that preincubation of apo-rCPO with vanadate gives identical behavior, indicating that the activation during turnover observed in trace a is not a consequence of reaching an equilibrium between apo-rCPO and vanadate. Therefore, indeed another component present during turnover must be responsible for this activation. Trace c shows that the presence of H_2O_2 is essential. After 4 min preincubation of the apo-rCPO with vanadate and H_2O_2, a higher initial rate is obtained which is identical to the rate observed after 4 min of turnover in trace a. These results show that the presence of H_2O_2 causes the activation of rCPO during turnover observed in trace a. Preincubation of the apo-enzyme with H_2O_2 in the absence of vanadate had no effect on activation behavior (not shown), indicating that the combination of vanadate and H_2O_2 is essential for this activation. We suggest that under the conditions used

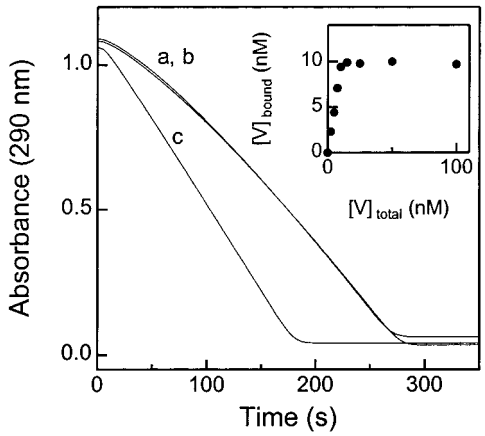

FIGURE 7: Enhanced cofactor binding during turnover of rCPO. Trace a: Activity assay containing 10 nM apo-rCPO, 10 nM vanadate, 50 mM MES, pH 5.0, and 50 μM MCD. The reaction was started by addition of 1 mM H_2O_2 and 5 mM Cl^-. Trace b: Same conditions as in trace a, but the reaction was started after 10 min preincubation of apo-rCPO and vanadate. Trace c: Same conditions as in trace a; reaction started after 4 min preincubation of apo-rCPO, vanadate, and H_2O_2. Inset: Titration of 10 nM apo-rCPO with pervanadate. Conditions: 100 mM citrate, pH 5.0, 1 mM H_2O_2. The reaction was started by the addition of 5 mM Cl^- after 25 min of preincubation.

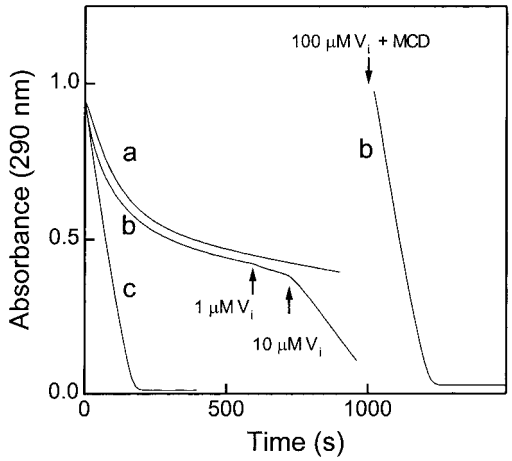

FIGURE 8: Inactivation of K353A during turnover. Trace a: 10 nM apo-K353A was mixed with 1 μM vanadate, 10 mM H_2O_2, and 40 mM Br^-. Trace b: 10 nM apo-K353A was first preincubated for 5 min with vanadate and H_2O_2 after which the reaction was started by addition of Br^-. At 10, 12, and 15 min 1, 10, and 100 μM vanadate was added, respectively. Trace c: 10 nM apo-K353A was mixed with 100 μM vanadate, 10 mM H_2O_2, and 40 mM Br^-.

pervanadate is present and that the apo-enzyme has a higher affinity for pervanadate than for vanadate. The activation phenomenon is also seen for the apo-enzyme from *C. inaequalis* (not shown), excluding the possibility that this effect is due to the recombinant system.

The incorporation of pervanadate is expected to be faster at high pervanadate concentrations, which was also observed (not shown). The dissociation constant for vanadate in the presence of H_2O_2 was investigated by preincubation of 10 nM apo-rCPO with various amounts of vanadate in the presence of H_2O_2 for 25 min, after which the chlorinating reaction was measured by the addition of 5 mM Cl^-. The amount of bound vanadium was calculated from the enzyme activity, assuming that maximal activity corresponds to 100% binding of vanadate to the apo-enzyme. This assumption was confirmed by the fact that this maximal activity (25 units/mg) was of similar magnitude as the maximal activity previously reported for this enzyme (*19*). The inset in Figure 7 shows that vanadate binds almost stoichiometrically to 10 nM apo-enzyme in the presence of H_2O_2. This indicates a dissociation constant for pervanadate of less than 5 nM at the optimal pH for this enzyme. A similarly small dissociation constant is found at pH 6 (not shown). Precise determination of the dissociation constant for peroxovanadate proved impossible due to contamination of glassware with trace amounts of vanadate, which results in a background rate which becomes too high as the apo-enzyme concentration is lowered. The very small value of the K_d for vanadate observed in the presence of H_2O_2 means that the determination of the K_d for vanadate, as carried out previously (*3*) by measuring the haloperoxidase activity, is obscured by a peroxovanadate contribution to the measured activity as a function of the vanadate concentration. This contribution was confirmed by comparing the activity of 10 nM apo-rCPO plus 10 nM vanadate (Figure 7, trace a) with the activity of a preincubation of 100 nM apo-rCPO plus 100 nM vanadate which was diluted 10 times in an activity assay. The activity of the 100 nM preincubation is significantly higher, indicating that vanadate indeed binds to the apo-enzyme in the 100−1000 nM range at pH 8.3 in the absence of H_2O_2. The pervanadate contribution implies that the K_d for vanadate is in fact somewhat higher than previously reported (*3*).

Effects of Mutations on Cofactor Binding during Turnover. As observed for rCPO, at low vanadate concentrations the activity of the mutants increases during turnover, making determination of the K_d for vanadate of the mutants difficult. Only for R360A could an upper limit of 20 μM be estimated from the optical absorbance experiments. K353A shows more complicated behavior in activity measurements as is shown in Figure 8. Trace a shows the result of immediate mixing of apo-K353A with 1 μM vanadate, H_2O_2, and Br^-. The rate is 13 s^{-1}, but inactivation occurs rapidly, and at $t = 10$ min, less than 10% of the initial activity is left. Preincubation with vanadate in the presence of H_2O_2 (trace b) resulted in a faster initial rate of 28 s^{-1}, showing that K353A has a higher affinity for vanadate in the presence of H_2O_2, as in the wild type. However, inactivation is observed again. As observed in trace c, only very minor inactivation occurs at a vanadate concentration of 100 μM. The inactivation requires the presence of all components required for turnover. Inactivation is especially prominent at low vanadate concentrations, and it was tested (trace b) whether the inactivation could be reversed by addition of vanadate. Ten minutes after the start of the reaction, 1 μM vanadate was added, which only slightly affected the activity. After 12 min, 10 μM was added, which induced partial reactivation, but the activity is still only 50% of the initial rate at 1 μM vanadate without prior inactivation (trace a). About 80% of the activity could be restored by addition of 100 μM vanadate (and 50 μM MCD), as compared to the initial rate of 100 μM without prior inactivation (trace c). In R360A these effects are qualitatively the same (not shown); inactivation is somewhat faster, but it can be fully reversed by addition of excess cofactor. Full inactivation of both K353A and R360A is observed after multiple turnovers as judged by comparing the amount of inactivated mutant with the amount of consumed monochlorodimedone.

Experiments similar to those in Figure 7 to determine the K_d for vanadate in the presence of H_2O_2 were also carried out for K353A and R360A. However, the inactivation at low vanadate concentrations as observed in Figure 8 takes place during the time required to obtain substantial absorbance differences in the monochlorodimedone assay, hampering the determination of the K_d. Nevertheless, the experiments indicate a K_d value much smaller than 50 nM (not shown), which is still strong binding. R490A shows similar activation during turnover; however, estimation of a K_d for pervanadate is further complicated by the fact that activation is primarily dependent on the presence of H_2O_2 but slow further activation is observed which requires all turnover components. It was not possible to reach a maximal activity for this mutant in a vanadate concentration range of 10 nM−500 μM.

DISCUSSION

The presence of a band in the optical absorbance spectrum of VCPO is in line with a previous report on a band in the UV−visible absorption spectrum of VBPO from *A. nodosum* (*13*). The production of large amounts of pure recombinant CPO in combination with the possibility of obtaining concentrated enzyme samples enables easy measurement of the UV absorbance of bound cofactor, which differs clearly in its optical properties from free vanadate. The absorbance maximum of 315 nm at pH 8.3 and 305−310 nm at pH 5.0 is similar to that reported for VBPO (315 nm). Upon addition of H_2O_2, an absorbance decrease is observed. A sharp intersection point (inset of Figure 3) indicates high affinity for H_2O_2. The peroxo species with a small absorption band at 384 nm that is formed is most likely the same species as observed in the crystal structure of the enzyme after addition of H_2O_2 at pH 8.3 (*10*). The origin of the observed absorbance at 315 nm in the UV−VIS spectrum of holo-CPO and the 384 nm peak in the peroxo form remains unclear. It has been reported that the UV absorbance of vanadate shifts to higher wavelength upon complex formation with an amine derivate (*26*) and also in vanadium (V) alkoxo complexes (*27*). The complexes of vanadium (V) with nitrogen-coordinating ligands in these studies may be regarded as analogous structures to the vanadate−His496 unit in VCPO. Free vanadate also exhibits a UV absorbance that decreases upon addition of H_2O_2 (Figure 3), but its position at about 270 nm is shifted to higher wavelength when vanadate is incorporated into the enzyme. Its intensity is also greater when bound to the enzyme. The optical spectra of the mutants described in this paper demonstrate that the presence of His496 is essential for the optical band of holo-CPO and that Arg360 influences this band but is not essential. The importance of Arg490 and Lys353 for this band is not clear, since the optical band in the spectra of R490A and K353A is missing, suggesting that vanadate does not bind to these mutants. Crystal structures of these mutants are not available. It could be argued that the fact that activity is observed for these mutants means that vanadate does bind (*9*); however, this activity only proves that vanadate binds to the K353A and R490A mutants in the presence of H_2O_2 and not necessarily in the absence of H_2O_2. This could indicate that these mutants have a high affinity for pervanadate and not for vanadate. In studies of dioxovanadium model compounds for VHPO's, positive absorption bands in the visible region (~450 nm) could be detected upon reaction with H_2O_2, requiring high concentrations of the vanadium(V) compound and H_2O_2 (*28, 29*). In analogy to these model compound studies, the positive peak of the peroxo form can be attributed to a peroxo-to-vanadium charge-transfer band.

The stopped-flow experiments presented in this paper show that binding of H_2O_2 to the enzyme is very fast at pH 8.3 and slower at pH 5.0, in line with the estimated k_{cat}/K_m values presented in this paper and previously reported (*11, 30*). At pH 5.0, the peroxo intermediate is unstable when 1 equiv of H_2O_2 is used. This is not due to catalase activity, but probably rather to the presence of traces of halide. The pseudo-first-order data show that the binding of H_2O_2 is reversible at pH 5.0. Oxidation of chloride by the peroxo intermediate does not appear to be reversible (Figure 6, inset), but a (fast) preequilibrium between the peroxo form and chloride may explain the hyperbolic dependence of the observed rate constant upon chloride concentration. These data clearly confirm that oxidation of chloride is the rate-determining step in catalysis, which was anticipated since bromide oxidation by the same peroxo intermediate is nearly 1 order of magnitude faster (*9, 19*).

Very surprisingly, the activity measurements presented in this paper (Figure 7) indicate that the cofactor is bound much more strongly in the peroxo form of the enzyme than in the native form. The estimated K_d for vanadate in the presence of H_2O_2 at pH 5.0 (less than 5 nM) is much lower than the K_d estimated for vanadate in the absence of H_2O_2 [100−1000 nM at pH 8.3 and >1 μM at pH 5.0 (*3*)]. Physiologically, the very small K_d for vanadate in the presence of H_2O_2 would mean that much lower concentrations of vanadate can be used effectively by the enzyme if a significant H_2O_2 concentration is present in vivo. Recently, it was found that VCPO is related to a large family of acid phosphatases and that the apo-enzyme exhibits phosphatase activity in vitro (*4*−*6*); it is therefore conceivable that the enzyme acts as a phosphatase in vivo. However, the turnover rate for the artificial phosphatase substrate *p*-nitrophenyl phosphate is only 1.7 min^{-1} (*6*), and our finding that the enzyme has a very high affinity for vanadate in the presence of H_2O_2 gives further evidence that the enzyme acts as a peroxidase in vivo. Our findings also suggest that pervanadate will bind more strongly to the phosphatases that share a common active site with CPO and thus should be more strongly inhibited by vanadate in the presence of H_2O_2. One of these phosphatases is human G6Pase (*6*). In this respect, it is interesting that studies have established that vanadate has an insulin mimetic effect (lowering glucose levels in blood) (*31, 32*), although the mechanism by which this occurs remains controversial. It is likely that the mechanism involves the inhibition of a phosphatase, since vanadate binds strongly to the active site of these enzymes, resulting in a pentacoordinated structure that mimics the transition state of these nonmetal phosphatases (*10, 33*). It has also been shown that pervanadate has a much stronger insulin mimetic effect than vanadate (*34, 35*).

It was previously suggested that inhibition of G6Pase could contribute to the insulin mimetic effect of vanadate (*16*), and recent papers (*15, 36*) also suggest that the main target of vanadate and peroxovanadate may be G6Pase, which would be in line with our observation that peroxovanadate binds more strongly to CPO. The study by Sekar et al. using rat adipocytes shows that vanadate strongly inhibits the dephos-

phorylation of endogenously formed glucose 6-phosphate, with an inhibition constant of 7 μM. The inhibition of G6Pase has a double glucose-lowering effect, since glucose 6-phosphate is an allosteric activator of glycogen synthase (*37*). Westergaard et al. characterized the inhibitory effect of peroxovanadium compounds and vanadate on isolated microsomal G6Pase (*15*), and found that the peroxovanadium compounds were very potent inhibitors (K_i 0.21−0.96 μM), a clearly stronger inhibition than vanadate (K_i 20.0−20.3 μM). In vivo effects also led them to conclude that the peroxovanadium compounds have a direct effect on the G6Pase. Molybdate and tungstate also have insulin mimetic effects, although higher concentrations are needed for the same effect as vanadate (*38*). Since it has been shown that the apo-BPO from the seaweed *Ascophyllum nodosum*, which is homologous to G6Pase (*6*), binds molybdate less strongly than vanadate (*39*), this would be in agreement with the weaker inhibition of G6Pase by this compound. In addition, the crystal structure of apo-CPO complexed with tungstate (*40*) shows that no covalent bond is formed between tungstate and His496 as is observed for vanadate in the holo-enzyme. It is likely that a similar difference in binding to the corresponding His176 in G6Pase (*6*) is the structural basis for the putative lower affinity for tungstate as compared to vanadate. If the hypothesis that G6Pase is a key target for these compounds in establishing the insulin mimetic effect is correct, then a possible negative side effect of pervanadate-inhibited G6Pase could be the creation of peroxidase activity, either direct (*41*, *42*) or via the oxidation of halides.

The nature of the reversible inactivation of the VCPO mutants R360A and K353A during turnover (Figure 8) is not clear. The possibility that a residue which is essential for activity is oxidized under turnover conditions with a high H_2O_2 concentration as shown for VBPO from *A.nodosum* (*43*) is not likely in this case since this would lead to irreversible inactivation. Since the inactivation is faster at low vanadate concentrations and can be largely restored by addition of this cofactor, we suggest turnover-induced modification of a residue (which is essential for the binding of vanadate but not for activity) is responsible for the observed inactivation. In principle, another option is modification of the cofactor itself, although it is not clear what the nature of this inactivation would be.

In conclusion, we have shown that the binding of vanadate to chloroperoxidase from *C. inaequalis*, the binding of H_2O_2, and the oxidation of Cl^- can be followed by UV−visible absorption spectroscopy. For vanadium haloperoxidases, this is the first time that individual kinetic steps in the reaction mechanism can be examined spectroscopically. Furthermore, we have shown that the binding of vanadate is strongly enhanced by the presence of the substrate H_2O_2, which could be physiologically important. The observation that the binding of pervanadate is much stronger than vanadate in VCPO predicts similar inhibitory effects for pervanadate in related acid phosphatases such as human G6Pase. The latter effect could explain the enhanced insulin mimetic effects of peroxovanadium compounds.

ACKNOWLEDGMENT

We thank Dr. Maarten Merkx for stimulating discussions and useful comments, Dr. Simon de Vries for the use of the stopped-flow apparatus, and Prof. Dr. Bruce Averill for reading the manuscript.

REFERENCES

1. De Boer, E., and Wever, R. (1988) *J. Biol. Chem. 263*, 12326−12332.
2. Arber, J. M., De Boer, E., Garner, C. D., Hasnain, S. S., and Wever, R. (1989) *Biochemistry 28*, 7968−7973.
3. Van Schijndel, J. W. P. M., Simons, L. H., Vollenbroek, E. G. M., and Wever, R. (1993) *FEBS Lett. 336*, 239−242.
4. Stukey, J., and Carman, G. M. (1997) *Protein Sci. 6*, 469−472.
5. Neuwald, A. F. (1997) *Protein Sci. 6*, 1764−1767.
6. Hemrika, W., Renirie, R., Dekker, H. L., Barnett, P., and Wever, R. (1997) *Proc. Natl. Acad. Sci. U.S.A. 94*, 2145−2149.
7. Hemrika, W., and Wever, R. (1997) *FEBS Lett. 409*, 317−319.
8. Pan, C. J., Lei, K. J., Annabi, B., Hemrika, W., and Chou, J. Y. (1998) *J. Biol. Chem. 273*, 6144−6148.
9. Hemrika, W., Renirie, R., Macedo-Ribeiro, S., Messerschmidt, A., and Wever, R. (1999) *J. Biol. Chem. 274*, 23820−23827.
10. Messerschmidt, A., Prade, L., and Wever, R. (1997) *Biol. Chem. 378*, 309−315.
11. Van Schijndel, J. W. P. M., Vollenbroek, E. G. M., and Wever, R. (1993) *Biochim. Biophys. Acta 1161*, 249−256.
12. Hormes, J., Kuetgens, U., Chauvistre, R., Schreiber, W., Anders, N., Vilter, H., Rehder, D., and Weideman, C. (1988) *Biochim. Biophys. Acta 956*, 293−299.
13. Tromp, M. G., Olafsson, G., Krenn, B. E., and Wever, R. (1990) *Biochim. Biophys. Acta 1040*, 192−198.
14. Chasteen, N. D. (1983) in *Structure and Bonding*, pp 105−138, Springer-Verlag, Berlin and Heidelberg.
15. Westergaard, N., Brand, C. L., Lewinsky, R. H., Andersen, H. S., Carr, R. D., Burchell, A., and Lundgren, K. (1999) *Arch. Biochem. Biophys. 366*, 55−60.
16. Hemrika, W., Renirie, R., Dekker, H., and Wever, R. (1998) in *Vanadium Compounds. Chemistry, Biochemistry, and Therapeutic Applications* (Tracey, A. S., and Crans, D. C., Eds.) pp 216−227, Oxford University Press, New York.
17. Macedo-Ribeiro, S., Hemrika, W., Renirie, R., Wever, R., and Messerschmidt, A. (1999) *J. Biol. Inorg. Chem. 4*, 209−219.
18. Bradford, M. M. (1976) *Anal. Biochem. 72*, 248−254.
19. Barnett, P., Hemrika, W., Dekker, H. L., Muijsers, A. O., Renirie, R., and Wever, R. (1998) *J. Biol. Chem. 273*, 23381−23387.
20. Khan, A. U., and Kasha, M. (1963) *J. Chem. Phys. 39*, 2105.
21. Allen, R. C. (1975) *Biochem. Biophys. Res. Commun. 63*, 675−683.
22. Kanofsky, J. R. (1984) *J. Biol. Chem. 259*, 5596−5600.
23. Soedjak, H. S., and Butler, A. (1990) *Biochemistry 29*, 7974−7981.
24. Fersht, A. (1985) in *Enzyme Structure and Mechanism*, pp 121−154, W. H. Freeman and Company, New York.
25. Cornish-Bowden, A. (1995) *Analysis of Enzyme Kinetic Data*, Oxford University Press, New York.
26. Crans, D. C., and Shin, P. K. (1988) *Inorg. Chem. 27*, 1797−1806.
27. Carrano, C. J., Mohan, M., Holmes, S. M., De la Rosa, R., Butler, A., Charnock, J. M., and Garner, C. D. (1994) *Inorg. Chem. 33*, 646−655.
28. Hamstra, B. J., Colpas, G. J., and Pecoraro, V. L. (1998) *Inorg. Chem. 37*, 949−955.
29. Colpas, G. J., Hamstra, B. J., Kampf, J. W., and Pecoraro, V. L. (1996) *J. Am. Chem. Soc. 118*, 3469−3478.
30. Van Schijndel, J. W. P. M., Barnett, P., Roelse, J., Vollenbroek, E. G. M., and Wever, R. (1994) *Eur. J. Biochem 225*, 151−157.
31. Meyerovitch, J., Farfel, Z., Sack, J., and Shechter, Y. (1987) *J. Biol. Chem. 262*, 6658.
32. Heyliger, C. E., Tahiliani, A. G., and McNeill, J. H. (1985) *Science 227*, 1474−1476.

33. Lindqvist, Y., Schneider, G., and Vihko, P. (1994) *Eur. J. Biochem. 221*, 139−142.
34. Fantus, G. I., Kadota, S., Deragon, G., Foster, B., and Posner, B. I. (1989) *Biochemistry 28*, 8864−8871.
35. Kadota, S., Fantus, I. G., Deragon, G., Guyda, H. J., Hersh, B., and Posner, B. I. (1987) *Biochem. Biophys. Res. Commun. 147*, 259−266.
36. Sekar, N., Li, J., He, Z., Gefel, D., and Shechter, Y. (1999) *Endocrinology 140*, 1125−1131.
37. Villar-Palasi, C. (1991) *Biochim. Biophys. Acta 1244*, 203−208.
38. Li, J., Elberg, G., Libman, J., Shanzer, A., Gefel, D., and Shechter, Y. (1995) *Endocrine 3*, 631.
39. De Boer, E., Boon, K., and Wever, R. (1988) *Biochemistry 27*, 1629−1635.
40. Messerschmidt, A., and Wever, R. (1998) *Inorg. Chim. Acta 273*, 160−166.
41. Andersson, M., Willetts, A., and Allenmark, J. (1997) *J. Org. Chem.*, 8455.
42. Ten Brink, H. B., Tuynman, A., Dekker, H. L., Hemrika, W., Izumi, Y., Oshiro, T., Schoemaker, H. E., and Wever, R. (1998) *Inorg. Chem. 37*, 6780−6784.
43. Meister Winter, G. E., and Butler, A. (1996) *Biochemistry 35*, 11805−11811.

BI9921790